Itaconic Acid-Based Hydrogels with Flame Retardancy and High-Temperature Resistance via Vat Photopolymerization 3D Printing

Rong Li[1], Runhao Yu[1], Chuan Liu[2], Kangan Hao[2], Anrong Huang[3], Chong Wu[4] and Xiaoling Zuo[1,*]

[1]*College of Materials Science and Engineering, Guizhou Minzu University, Guiyang 550025, China*

[2]*College of Physics and Mechatronic Engineering, Guizhou Minzu University, Guiyang 550025, China*

[3]*National Engineering Research Center for Compounding and Modification of Polymeric Materials, Guiyang 550014, China*

[4]*College of Pharmacy, Guizhou University of Traditional Chinese Medicine, Guiyang 550025, China*

Abstract: Biomass-based hydrogels have received extensive attention due to their flame retardant properties and environmental friendliness. The dilemma that non-renewable energy resources are increasingly depleted, leads us to place high expectations on renewable natural clean energy, as well as to conduct in-depth research on the efficient utilization and green preparation processes for the clean energy. In this study, we introduce a green and sustainable method for the design and preparation of flame-retardant materials by integrating two new class of itaconic acid-based hydrogels in conjunction with the rapid vat photopolymerization (VP) 3D printing technology. The hydrogels prepared by this method exhibit exceptional flame retardancy, mechanical robustness and superior high-temperature resistance. This research provides novel strategies and essential guidance for the green synthesis and sustainable development of next-generation flame retardant materials.

Keywords: Hydrogels, Itaconic acid, Flame retardancy, High-temperature resistance, 3D printing, Vat photopolymerization.

1. INTRODUCTION

Hydrogels, as a class of newly-developing flame-retardant materials, have tremendous potential for their applications in preventing coal-mine, forests, buildings and textile from fire [1-3]. Because water binding, cooling, and holding capabilities specific to hydrogels make them hold great promising in terms of fireproofing and extinguishing. Meanwhile, the high heat capacity and latent heat of vaporization of water endow hydrogels with the extraordinary abilities of declining thermal energy and stemming heat transfer [4-5].

The status quo of the gradually reduced petroleum-derived materials has leaded to the issues of various environmental problems and shortages of these commodities, which prompt the exploitation of renewable and sustainable materials to deal with this problem. Within this context, biomass materials have become a promising component to construct hydrogels, not only the superiorities of abundance, ecological sustainability and environmental friendliness [6-7]. More critically, the bearing of abundant hydroxyl groups within biomass materials, which can perform as an important carbon-forming agent, allows for their tremendous potential for the development of green flame-retardant materials [8]. Among many biomass materials, noteworthy one is itaconic acid (IA), an unsaturated dicarboxylic acid produced from lignocellulose biomass, is a promising alternative to petrochemical-based monomers as a building block for plastics, resins, and synthetic fibers [9-10]. The USA Department of Energy lists it as a top-12 value-added chemical produced from biomass [11]. However, the development of biomass-based hydrogels comprising itaconic acid with well-behaved flame resistance remains scarce.

Recent preparation methods of biomass-based hydrogels come at the price of long reaction time and high energy consumption, such as UV irradiation, thermal polymerizations and redox polymerizations [12-14], severely imposing restrictions on the further development of biomass-based hydrogels. Vat photopolymerization (VP) is a technology with a time-honored history, it also meets the requirement of nearly no release of volatile organic compounds, meanwhile, benefits from room temperature operation with the using of appropriate radiation sources [15-17]. Introducing VP technology into 3D printing encompasses several significant superiorities, including eco-friendly, energy saving, finer accuracy and satisfactory spatiotemporal control [18-19]. It is thus essential to advance VP 3D printing technology for the

*Address corresponding to this author at the College of Materials Science and Engineering, Guizhou Minzu University, Guiyang 550025, China;
E-mail: shanghai0401@163.com

E-ISSN: 1929-5995/24

fabrication of biomass-based hydrogels. However, there are still few reports on biomass-based hydrogels prepared via VP 3D printing, especially related to those itaconic acid-based hydrogels with flame retardancy [20].

To that end, we first develop a new class of biomass-based printing ink with efficient visible-light curing capabilities, principally composed of the renewable itaconic acid. The development of this printing ink aims to cope with the challenges derived from the slow visible-light curing process of biomass monomers, after all, which has been demonstrated by the previous work that biomass reactive monomers generally have a low photopolymerization efficiency even upon UV exposure [21]. We herein employ a commercial LCD 3D printer, which is assembled with a low intensity visible-light source (*i.e.,* LED @405 nm), to fabricate this class of itaconic acid-based hydrogels in a green and eco-friendly, efficient and controllable manner. Fourier Transform Infrared Spectroscopy (FTIR) and real-time FTIR (RT-FTIR) were employed here to confirm the structure and condensed phase products of itaconic acid-based hydrogels as well as to detect the polymerization kinetics of 3D printing ink. Limiting Oxygen Index (LOI), UL-94 and micro-scale combustion calorimetry (MCC) tests were utilized to character the flame retardancy of itaconic acid-based hydrogels. Further, Thermogravimetric Analysis (TGA) and universal testing machine were employed to examine the high-temperature thermal stability and mechanical properties of the hydrogels, respectively. These hydrogels have been demonstrated that they can exhibit satisfactory flame retardancy and excellent temperature resistance, providing inspiration for the development of the traditional flame-retarded materials toward high-performance and sustainability. More importantly, the approach to fabricating biomass-based hydrogels could further push this appealing halogen-free flame-retarded materials to applications of new heights.

2. MATERIALS AND METHODS

2.1. Materials

Itaconic acid (IA, 99%, M_W 130.10) and diphenyl(2,4,6-trimethylbenzoyl)phosphine oxide (TPO, 98%, M_W 348.38) were purchased from TCI Co., Ltd. (Shanghai, China). Triethanolamine (TEOA, 99%, M_W 149.19), polyvinylpyrrolidone (PVP, M_W 40,000) was obtained from Aladdin Chemistry Co., Ltd. (Shanghai, China). 4-Methoxyphenol (99%, M_W 190.22), 1,4-butanediol (99%), n-hexane (99%), *n*-butyl acetate (99%), sodium dodecyl sulfate (SDS, 99%), N,N-dimethylbenzylamine (99%), isopropyl alcohol (99%) and p-toluenesulfonic acid (99%) were obtained from Innochem Co., Ltd. (Beijing, China). Diglycidyl ether (PEGGE, 99%) were purchased from Macklin Biochemical Co., Ltd. (Shanghai, China). 2-Hydroxyethyl methacrylate (HEMA, water≤50 ppm, 99%) was gotten from Adamas Co., Ltd. (Shanghai, China). Epoxide resin E-51 (EP, epoxide number 0.48-0.52) was supplied by Mreda Co., Ltd. (Beijing, China).All the reagents and solvents were used as received without further purification.

2.2. Chemical Modification of Itaconic Acid

Itaconic acid (2.248 g), N,N-dimethylbenzylamine (0.021 g) and 4-methoxyphenol (0.023 g) were dissolved in the co-solvent, 2-hydroxyethyl methacrylate (2.5 g), and then the solution was heated and stirred at 80 °C. The mixture of epoxide resin (2.1 g) and poly(ethylene glycol) diglycidyl ether (2.47 g) was added into the aforementhioned solution within 0.5 h after stirring for 3 h at room temperature. Subsequently, the solution was stirred and heated at 105 °C for 3 h. The liquid products with light yellow IAE were obtained after the reaction. The synthetic route of IAE is shown in Scheme **S1**.

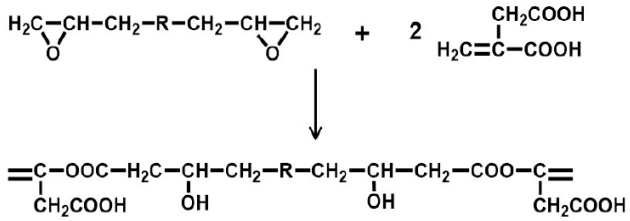

Wherein R represents,

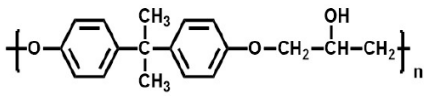

Scheme 1: The synthetic route of IAE.

Itaconic acid (7.8 g), 1,4-butanediol (4.505 g) and p-toluenesulfonic acid (0.078 g) were stirred and heated at 130 °C for 4 h. The mixture was refluxed under a nitrogen atmosphere, the gas flow kept at 2-3 bubbles per second. Subsequently, 4-methoxyphenol (0.078 g) was added into the aforementhioned mixture and heated at 130 °C for another 2 h. The liquid products IAB with light yellow were obtained after the reaction and kept under 4 °C in dark.The synthetic route of IAB is shown in Scheme **2**.

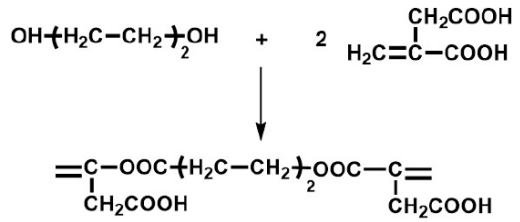

Scheme 2: The synthetic route of IAB.

2.3. Preparation of Photoinitiator (PI) Nanoparticles

Based on the previously reported method for preparing photoinitiator nanoparticles [22], oil-in-water microemulsions containing TPO (1.7 g) were prepared at room temperature by mixing 25.2 mL *n*-Butyl acetate with SDS (7.5 g), PVP (7.5 g) and 26.8 mL isopropyl alcohol to create an organic phase in which TPO was dissolved. Whereafter, the organic phase was mixed with 40.0 mL deionized water and magnetically stirred until clear systems were obtained. The solvent was removed by rotary evaporator to obtain the crude product.

2.4. 3D Printing of Hydrogels

The IAE and IAB hydrogels were prepared by an aqueous solution containing IAB or IAE monomer and TEOA with photoinitiator TPO nanoparticles. The IAE/IAB hydrogel was prepared by an aqueous solution containing IAB monomer, IAE monomer, TEOA and TPO nanoparticles. The detailed weight of each composition is listed in Table **1**. Afterward, the printing ink for IAE, IAB and IAE/IAB hydrogels was thoroughly stirred at room temperature for 24 h. Note that TEOA plays a role of neutralizer in adjusting the pH to 7.

A predesigned cuboid hydrogel was 3D printed using a LCD 3D printer (LD-006, Creality) with a 405 nm LED light source (λ: 375-435 nm, irradiance = 14.5 $mW \cdot cm^{-2}$). This printer was operated by a top-down LCD system with a digital mirror device. A designed 3D model was first sliced into a series of 2D images. During the printing, the parameter of base layers was set to 10. Regarding hydeogels, the sliced thickness of each layer was set to 20 μm, the exposure time was set to approximately 7 s for the first layer, and the exposed time of each layer was 5 s. After printing, the obtained hydrogels were rinsed with water in a sonicator bath for 2 min to remove the monomers/photoinitiator residues and additives. The printed hydrogels were stored in a sealed environment with a high moisture content to prevent excessive water evaporation.

2.5. Characterization

2.5.1. Characterization of Structural Features and Polymerization Kinetics

Proton nuclear magnetic resonance spectroscopy (^{1}H NMR) spectra of IAB and IAE were recorded on a Bruker Advance AMX-400 Spectrometer in CD_4O. The evolution of the double bond content of 3D printing ink was continuously followed by real-time fourier transform infrared reflection (RT-FTIR) spectroscopy (JASCO FTIR 4100) in the range of 870-970 cm^{-1}. Polymerization kinetics were assessed *in situ* by integrating the attenuance of the double-bond vibrational bands during 405 nm LED irradiation [18]. The infrared spectra of the hydrogels in dry state were recorded by attenuated total reflectance Fourier transform infrared spectroscopy. While the variations of the chemical structures of residue chars heated by different temperatures (10 min) were recorded by Fourier transform infrared spectroscopy using KBr pellets. During the testing process, the samples quality had a constant value, and the quality proportion of the samples to KBr was fixed [23]. The spectra were obtained with 16 scans and a resolution of 4 cm^{-1} in the range of 4000-500 cm^{-1} at room temperature.

2.5.2. Characterization of Flame Retardancy and Combustibility

Firstly, the hydrogels were placed in a constant temperature and humidity chamber (25 °C, relative humidity (RH) 65 %) for 24 h before testing. The flame retardancy of all hydrogels was evaluated by limiting oxygen index (LOI) and UL-94 tests. The LOI value was surveyed on a JF-3 oxygen index meter

Table 1: The Compositions of IAE/IAB Hydrogel

Weight (g)	DIW	IAB	IAE	TPO nanoparticles	TEOA
IAE hydrogel	50	NA	40	4	12
IAB hydrogel	50	70	NA	7	20
IAE/IAB hydrogel	50	70	40	11	32

Notes: DIW stands for Deionized Water.

(Jiangning, China) with the dimensions of 80 × 10 × 4 mm^3 in accordance with the ASTM D2863-2006 [24]. LOI analysis was tested three times repeatedly to obtain the average values in this work. The UL-94 test was performed according to ASTMD 3801 on a SH5300 instrument (Guangzhou, China). The specimens used for this test were of the dimensions of 130 × 13 × 3.2 mm^3 [25].

The micro-scale combustion calorimetry (MCC) test was carried out on FAA-PCFC (Fire Testing Technology Limited) according to ASTM D7309-21a under a relative humidity 50 ± 5% at 25 ± 2 °C [26]. The LOI and MCC values were the average of three measurements and the results were considered to be reproducible to ± 10%.

2.5.3. Characterization of Morphology Features

SEM images obtained on KYKY-2800B (KYKY Technology Development, China) were used to investigate the residue chars after LOI tests for all hydrogels with an acceleration voltage of 20 KV. All samples were recorded after gold coating surface treating.

2.5.4. Characterization of Thermal Stability and Decomposition

Thermogravimetric analysis/infrared spectrometry (TG-IR) spectra of all hydrogels in dry state were studied by a TG analyzer (STA 449 C, Germany) equipped with an infrared spectrometer (Tensor 27, Germany) from room temperature to 600 °C at a heating rate of 20 °C/min under nitrogen atmosphere to investigate the gas components resulting from thermal decomposition. About 10 mg of each of the sample was loaded in a platinum sample pan. The TGA values were the average of three measurements and the results were considered to be reproducible to ± 10%.

2.5.5. Characterization of Mechanical Strength

Tensile strength-strain tests were carried out with a commercial electronic universal tensile stress tester (WDW-10) with a 50 N load cell, in accordance with GB/T1040-2006 standards. The hydrogels were printed into standard dumbbell shapes with 2 mm thickness, 5 mm width, and 70 mm gauge length. The original hydrogels were kept in chambers with certain relative humidity and temperature till they reached their steady states. Then uniaxial tensile tests were performed immediately at a rate of 20 mm/min using a tensile machine. Each parameter was the average of five measurements.

3. RESULTS

Considering that the specially designed monomers IAE and IAB, which primarily contain itaconic acid, are solely soluble in neutral aqueous solution. So we utilized TEOA as a neutralizer to adjust the pH of IAE and IAB solution. The chemical structures of IAE and IAB are verified by ^1H NMR in Figure **S1** (Supporting Information). The photopolymerization profiles of 3D printing ink for the fabrication of IAE, IAB and IAE/IAB hydrogels are described in Figure **1a**. From the one-component printing ink, which is composed of IAE or IAB and TEOA and photoinitiator LAP, a double-bond final conversion (FC) of 40.9 % and 37.8 % is found after 600 s of 405 nm LED exposure, respectively. The combination of IAE- and IAB-based monomers leads to the increased viscosity of two-component printing ink [27], effectively reducing the impact of oxygen inhibition in contrast to one-component printing ink. A conversion

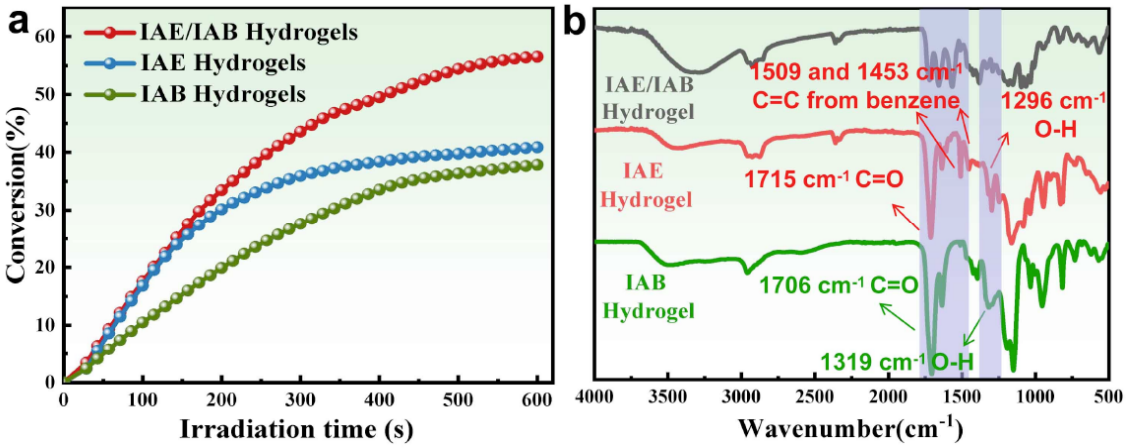

Figure 1: (**a**) Alkene function conversions versus time of different 3D printing ink for the fabrication of biomass-based hydrogels in air under 405 nm LED irradiation. (**b**) The FTIR spectra of different freeze-dried hydrogels.

maximum equal to 56.5 % after 600 s of visible-light irradiation is thus obtained for the alkene functions of two-component printing ink. The successful fabrication of IAE/IAB hydrogel can be confirmed by the absorption peaks of C=O (at around 1710 cm^{-1}) and O-H (at around 1300 cm^{-1}) of IAE and IAB hydrogels, respectively. Besides, the absorption peaks of C=C of bezene at 1453 and 1509 cm^{-1} can also be found within IAE/IAB hydrogel. From this, we can conclude that VP 3D printing technology is beneficial to prepare biomass-based hydrogels with the advantages of green and efficiency.

From the stress-strain curves shown in Figure **2a** and the corresponding data summarized in Table **S1**, the stress is measured as 87.4 KPa and 95.2 KPa for IAE and IAB hydrogels, respectively. As expected, inspiring result of IAE/IAB hydrogel was favourably achieved according to the combination of IAE and IAB hydrogels. Clearly, the stress increases with the introduction of IAB into IAE hydrogels, which is measured up to 170.1 KPa. In addition, the highly ordered layer-by-layer packing structures, typical architecture of 3D-printed materials, have been demonstrated to be a major factor to enhance the mechanical properties of biomass-based hydrogels [4]. The typical TGA and DTG curves of IAE/IAB hydrogel are exhibited in Figure **2b** and summarized in Table **S2**. The thermal stability investigated for IAE/IAB hydrogel presents that except the water loss occurred at about 83 °C, the values of maximum degradation temperature (T_{max}) gather in a temperature range of 300-420 °C, meanwhile, accompanied by a value of 4.0% residues in the high-temperature region, demonstrating the fine thermal stability possessed by IAE/IAB hydrogel.

High-temperature resistance, which indicates the capability of withstanding the enormous thermal shock associated with extreme environments, is the other critical parameter to evaluate the thermal stability of materials [1]. Figure **3a** shows time-dependent temperature profiles of IAE/IAB hydrogel. The hydrogel with thickness of 5mm was placed over an alcohol burner with about 600 °C of flame temperature, the space between them was fixed at 50 mm. IAE/IAB hydrogel exhibits excellent high-temperature resistance that its surface temperature rises with the heating time and only reaches about 82.5 °C after 630 s of heating. It is clear that IAE/IAB hydrogel shows a low pyrolysis rate during the process of heating and a well-behaved thermal insulating ability. Therefore, the photos in Figure **3b** illustrate that IAE/IAB hydrogel nearly maintained the original appearance with a surface temperature of 59.9 °C after 360s of heating, and, the fresh flowers and leaves could be well protected by IAE/IAB hydrogel even at such high temperature. After 630 s of heating, only a slight carbonization phenomenon was detected in marginal part of IAE/IAB hydrogel, meanwhile, the fleabanes were slightly dehydrated, suggestive of the outstanding thermal protection ability possessed by IAE/IAB hydrogel.

Turning to the flame performance, a LOI value of about 56.8 % and the optimal UL 94-V0 rating are found for IAE/IAB hydrogel, indicative of the outstanding flame retardancy for this class of itaconic acid-based hydrogel. The detailed parameters are collected in Table **S3**. Heat release rate (HRR) curve of IAE/IAB hydrogel versus temperature is depicted in Figure **4a**. The peak of HRR (pHRR) achieves a maximum value of 59.5 W/g at 430 °C, the other two lower pHRRs are found with values of 35.0 W/g (330 °C) and 18.8 W/g (244 °C) in the low-temperature

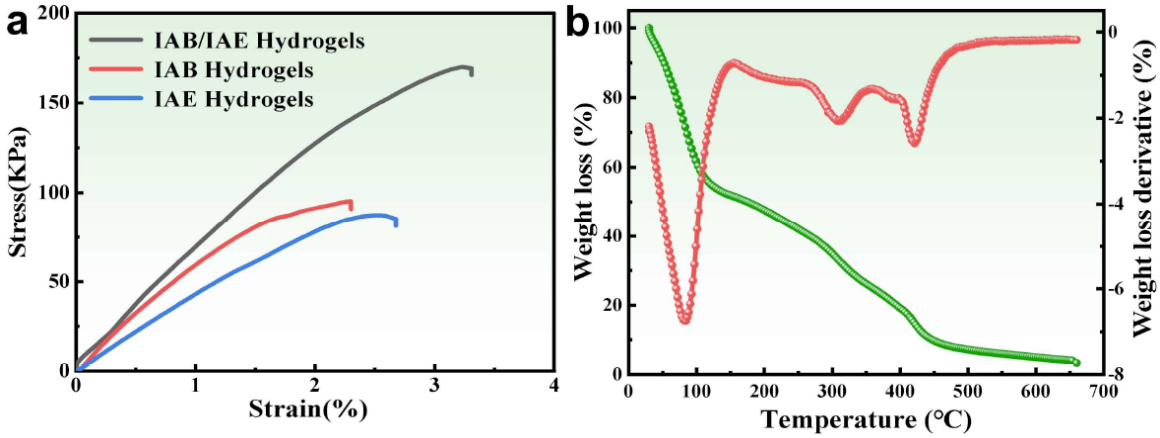

Figure 2: (**a**) Stress-strain curves for 3D-printed hydrogels. (**b**) Thermogravimetric analysis (TGA) and derivative thermogravimetry (DTG) curves of IAE/IAB hydrogel.

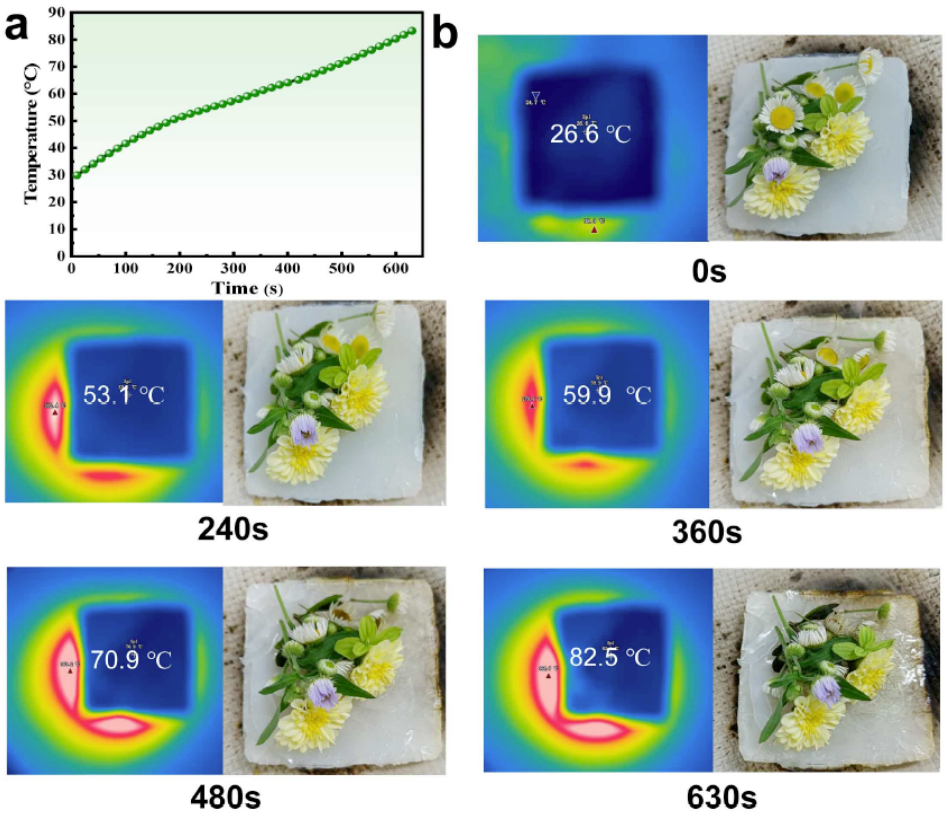

Figure 3: (**a**) Center temperature profiles of IAE/IAB hydrogel surfaces (tested by an infrared imager (Fortric 226S) once every 5 s). (**b**) Infrared and digital images of IAE/IAB hydrogel after different time of heating.

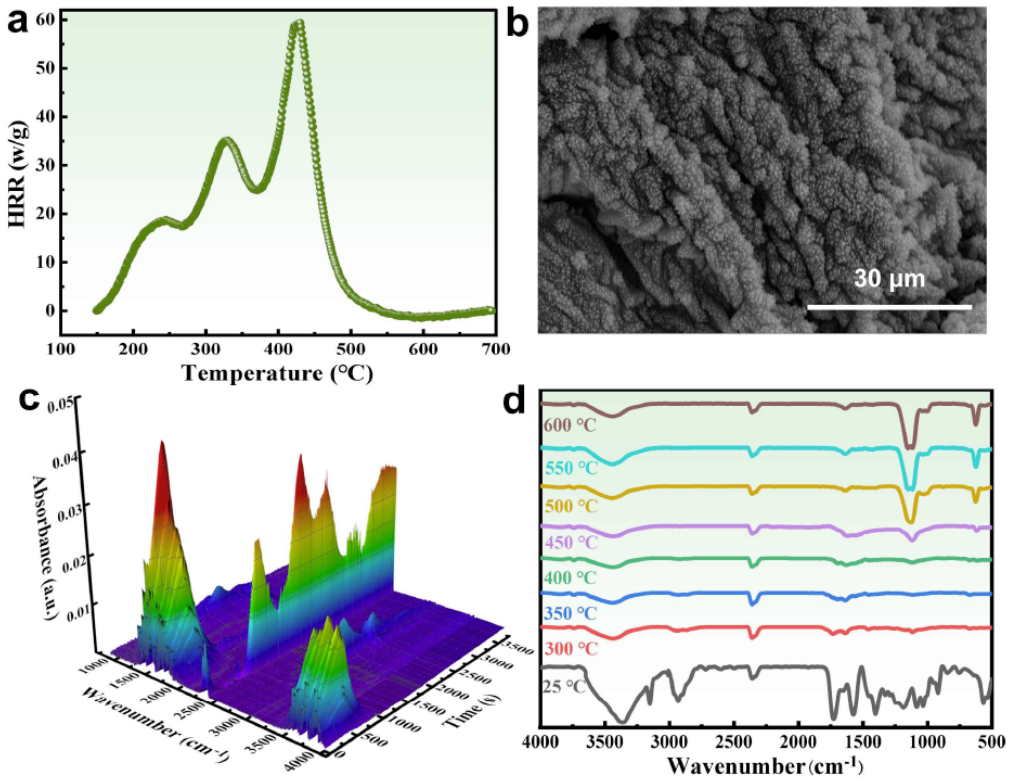

Figure 4: (**a**) Heat release rate (HRR) curve of IAE/IAB hydrogel. (**b**) SEM image of the residual chars after LOI test for IAE/IAB hydrogel. (**c**) FTIR spectra of the volatile gases from IAE/IAB hydrogel. (**d**) FTIR spectra of the condensed products of IAE/IAB hydrogel at different temperatures.

region, respectively. The morphology of residual chars in Figure **4b** demonstrates that the well-distributed and compact chars can be obtained from the IAE/IAB hydrogel after burning, agreement well with the well-behaved flame retardancy results of IAE/IAB hydrogel.

The gaseous products released by IAE/IAB hydrogel during thermal decomposition were analyzed by TG-IR. With the curves shown in Figure **4c**, one can see that water (3737 cm^{-1}), hydrocarbons (2950 cm^{-1}), carbon dioxide (2360 cm^{-1}), carbonyl compounds (1788 cm^{-1}), and ethers (1084 cm^{-1}) are the main decomposition products of IAE/IAB hydrogel [4]. In particular, the nonflammable gases, i.e., CO_2 and H_2O, can simultaneously be produced in abundance. They come into sight at 108 and 50 °C, respectively. Besides, the characteristic absorption peaks of ethers, carbonyl and hydrocarbons groups generated by IAE/IAB hydrogel appear at 215, 174 and 187 °C, respectively. This result confirms that the flame retardancy of gaseous phase exerts positively effects on the early stage of burning. The condensed phase products of IAE/IAB hydrogel were characterized by FTIR. The C=O of carboxyl groups (1727 cm^{-1}) is completely consumed at 450 °C for IAE/IAB hydrogel via decarboxylation pattern (Figure **4d**) [28]. The characteristic C-O-C band at 1186 cm^{-1} cannot be detected for IAE/IAB hydrogel after 300 °C [29], meaning that water is not generated after this temperature region. It illustrates that the flame retardancy of condensed plays a significant role in the latter stage of burning.

4. CONCLUSIONS

This study proposes a straightforward and biocompatible strategy for the preparation of halogen-free flame-retardant materials. By employing VP 3D printing technology with low-intensity visible light, we successfully fabricated a new class of naturally biomass-based flame-retardant hydrogels. The resultant hydrogels demonstrated exceptional flame retardant properties, mechanical strength, and outstanding high-temperature resistance. Evidently, itaconic acid-born materials, as an emerging class of biomass-based hydrogels, offer innovative insights into the design and development of halogen-free flame-retardant materials. Moreover, VP 3D printing technology exhibits immense potential in the green fabrication of halogen-free flame-retardant materials, thereby laying a foundation for the widespread application of these materials in the flame-retardant field. Although the current research has established a solid foundation for the development of these materials, there is still scope to further optimize and expand their applications. Besides, addressing the issues that complicated synthesis process and limited duration of biomass-based hydrogels are identically crucial for their wider applications.

MATERIALS AND METHODS

Details of Materials and Methods are available in the Supplementary Materials.

ACKNOWLEDGEMENTS

Xiaoling Zuo is grateful for the financial supported by National Natural Science Foundation of China (No. 12304482), Guizhou Provincial Basic Research Program (Natural Science) ZK[2022] Major Project 029, Fund Project of Guizhou Minzu University (4D Printing Smart Materials Technological Innovative Talents Team, GZMUZK[2023]CXTD01).

CONFLICT OF INTEREST

The authors declare no competing financial interest.

SUPPLEMENTARY MATERIALS

The supplementary materials can be downloaded from the journal website along with the article.

REFERENCES

[1] Zhang HQ, Liu ZJ, Mai JP, Wang N, Liu HJ, Zhong J, Mai X. M. A smart design strategy for super-elastic hydrogel with long-term moisture, extreme temperature resistance, and non-flammability. Adv Sci 2021; 8: 2100320. https://doi.org/10.1002/advs.202100320

[2] Yang HB, Liu ZX, Chen H, Yue X, Ling ZC, Han ZM, Yin CH, Ruan YH, Zhao X, Zhou Z, Li DH, Xie S, Yang KP, Guan QF, Yu, SH. An all-natural fire-resistant bioinspired cellulose-based structural material by external force-induced assembly. Mater. Today Nano 2023; 23: 100342. https://doi.org/10.1016/j.mtnano.2023.100342

[3] Li YS, Hu XM, Cheng WM, Shao ZA, Xue D, Zhao YY, Lu W. A novel hightoughness, organic/inorganic double-network fire retardant gel for coal-seam with high ground temperature. Fuel 2020; 263: 116779. https://doi.org/10.1016/j.fuel.2019.116779

[4] Zuo XL, Zhou Y, Hao KA, Liu C, Yu RH, Huang AR, Wu C, Yang YY. 3D printed all-natural hydrogels: Flame-retardant materials toward attaining green sustainability. Adv Sci 2024; 11: 2306360. https://doi.org/10.1002/advs.202306360

[5] Cui XF, Zheng WJ, Zou W, Liu XY, Yang H, Yan J, Gao Y. Water-retaining, tough and self-healing hydrogels and their uses as fire-resistant materials. Polym Chem 2019; 10: 5151-5158. https://doi.org/10.1039/C9PY01015G

[6] Wang YY, Liang ZC, Su ZP, Zhang K, Ren JL, Sun RC, Wang XH. All-biomass fluorescent hydrogels based on biomass carbon dots and alginate/nanocellulose for biosensing. ACS Appl Bio Mater 2018; 1: 1398-1407. https://doi.org/10.1021/acsabm.8b00348

[7] Liu Y, Zhang AS, Cheng YM, Li MH, Cui YC, Li ZW. Recent advances in biomass phytic acid flame retardants. Polym Test 2023; 124: 108100. https://doi.org/10.1016/j.polymertesting.2023.108100

[8] Raj T, Chandrasekhar K, Naresh Kumar A, Kim S-H. Lignocellulosic biomass as renewable feedstock for biodegradable and recyclable plastics production: A sustainable approach. Renew Sust Energ Rev 2022; 158: 112130. https://doi.org/10.1016/j.rser.2022.112130

[9] Zhao ML, Lu XY, Zong H, Li JY, Zhuge B. Itaconic acid production in microorganisms. Biotechnol Lett 2018; 40: 455-464. https://doi.org/10.1007/s10529-017-2500-5

[10] Magalhães AI, Carvalho JC, Thoms JF, Silva RS, Soccol CR. Second-generation itaconic acid: An alternative product for biorefineries? Bioresource Technol 2020; 308: 123319. https://doi.org/10.1016/j.biortech.2020.123319

[11] Tomishige K, Yabushita M, Cao J, Nakagawa Y. Hydrodeoxygenation of potential platform chemicals derived from biomass to fuels and chemicals. Green Chemistry 2022; 24: 5652-5690. https://doi.org/10.1039/D2GC01289H

[12] Wang D, Wang Y, Li T, Zhang SW, Ma PM, Shi DJ, Chen MQ, Dong WF. A bio-based flame-retardant starch based on phytic acid. ACS Sustainable Chem Eng 2020; 8: 10265. https://doi.org/10.1021/acssuschemeng.0c03277

[13] Zhao XJ, Liang ZW, Huang YB, Hai Y, Zhong XD, Xiao S, Jiang SH. Influence of phytic acid on flame retardancy and adhesion performance enhancement of poly (vinyl alcohol) hydrogel coating to wood substrate. Prog Org Coat 2021; 16: 106453. https://doi.org/10.1016/j.porgcoat.2021.106453

[14] Xue Y, Yang F, Li JY, Zuo XH, Pan BL, Li MK, Quinto L, Mehta J, Stiefel L, Kimmey C, Eshed Y, Zussman E, Simon M, Rafailovich M. Synthesis of an effective flame-retardant hydrogel for skin protection using xanthan gum and resorcinol bis(diphenyl phosphate)-coated starch. Biomacromolecules 2021; 22: 4535-4543. https://doi.org/10.1021/acs.biomac.1c00804

[15] Zuo XL, Wu C, Yang L, Huang AR, Dong ZG, Wang TF, Xu F, Zhang DH, Guo JB, Yang YY. Fluorescent brighteners in thiol-acrylate polymerizations: Sunlight-cured coatings and LED-assisted multifuctional intelligent nanoparticles synthesis. Prog Org Coat 2020; 148: 105829. https://doi.org/10.1016/j.porgcoat.2020.105829

[16] Zuo XL, Wang SF, Zheng K, Wu C, Zhang DH, Dong ZG, Wang TF, Xu F, Guo JB, Yang YY. Fluorescent-brightener-mediated thiol-ene reactions under visible-light LED: A green and facile synthesis route to hyperbranched polymers and stimuli-sensitive nanoemulsions. Dyes Pigments 2021; 189: 109253. https://doi.org/10.1016/j.dyepig.2021.109253

[17] Abu-Abdoun II, Aale-Ali AA. Synthesis and applications of onium salts for photopolymerization reactions. Journal of Research Updates in Polymer Science 2024; 13: 27-33. https://doi.org/10.6000/1929-5995.2024.13.04

[18] Zuo XL, Wang SF, Zhou Y, Wu C, Huang AR, Wang TF, Yang YY. Fluorescent hydrogel actuators with simultaneous morphing- and color/brightness-changes enabled by light-activated 3D printing. Chem Eng J 2022; 447: 137492. https://doi.org/10.1016/j.cej.2022.137492

[19] Zhou Y, Hao KA, Liu C, Yu RH, Huang AR, Wu C, Yang YY, Zuo XL. 3D printed hydrogels with time/temperature-dependent photoluminescence for multi-information dynamic display. ACS Appl Polym Mater 2024; 6: 2012-2021. https://doi.org/10.1021/acsapm.3c02863

[20] Vahabi H, Gholami F, Tomas M, Movahedifar E, Yazdi MK, Saeb MR. Hydrogel and aerogel-based flame-retardant polymeric materials: A review. Journal of Vinyl and Additive Technology 2024; 30: 5-25. https://doi.org/10.1002/vnl.22041

[21] Xenikakis I, Tsongas K, Tzimtzimis EK, Zacharis CK, Theodoroula N, Kalogianni EP, Demiri E, Vizirianakis IS, Tzetzis D, Fatouros DG. Fabrication of hollow microneedles using liquid crystal display (LCD) vat polymerization 3D printing technology for transdermal macromolecular delivery. Int J Pharmaceut 2021; 597: 120303. https://doi.org/10.1016/j.ijpharm.2021.120303

[22] Pawar AA, Saada G, Cooperstein I, Larush L, Jackman JA, Tabaei SR, Cho N-J, Magdassi S. High-performance 3D printing of hydrogels by water-dispersible photoinitiator nanoparticles. Sci Adv 2016; 2: e1501381. https://doi.org/10.1126/sciadv.1501381

[23] Zuo XL, Zhang KZ, Lei Y, Qin SH, Hao Z, Guo JB. Influence of thermooxidative aging on the static and dynamic mechanical properties of long-glass-fiber-reinforced polyamide 6 composites. J Appl Polym Sci 2014; 131: 39594. https://doi.org/10.1002/app.39594

[24] Zuo XL, Song HS, Shao HJ, Aud MH, Wei T, Guo JB. Effects of OMMT on the aging behaviors of halogen-antimony flameretarded LGFPA6 composites: Flammability and thermal degradation. Thermochim Acta 2017; 653: 32-42. https://doi.org/10.1016/j.tca.2017.04.001

[25] Zuo XL, Shao HJ, Zhang DH, Hao Z, Guo JB. Effects of thermal-oxidative aging on the flammability and thermaloxidative degradation kinetics of tris(tribromophenyl) cyanurate flame retardant PA6/LGF composites. Polym Degrad Stabil 2013; 98: 2774-2783. https://doi.org/10.1016/j.polymdegradstab.2013.10.014

[26] Liu JR, Yu ZC, He HL, Wang YS, Zhao YH. A novel flame-retardant composite material based on calcium alginate/poly (vinyl alcohol)/graphite hydrogel: thermal kinetics, combustion behavior and thermal insulation performance. Cellulose 2021; 28: 8751-8769. https://doi.org/10.1007/s10570-021-04047-7

[27] Ligon SC, Husar B, Wutzel H, Holman R, Liska R. Strategies to reduce oxygen inhibition in photoinduced polymerization. Chem Rev 2014; 114: 557-589. https://doi.org/10.1021/cr3005197

[28] Xu YJ, Qu LY, Liu Y, Zhu P. An overview of alginates as flame-retardant materials: Pyrolysis behaviors, flame retardancy, and applications. Carbohyd Polym 2021; 260: 117827. https://doi.org/10.1016/j.carbpol.2021.117827

[29] Tang WF, Liang GQ, Wang L, Yuan Y, Dessie W, Liu F, Qin ZD, Wang Y, Xiao AG, Jin XD. Multi-functional flame retardant coatings comprising chitosan/ gelatin and sodium phytate for rigid polyurethane foams. J Clean Prod 2023; 394: 136371. https://doi.org/10.1016/j.jclepro.2023.136371

Received on 06-08-2024 Accepted on 02-09-2024 Published on 26-09-2024

https://doi.org/10.6000/1929-5995.2024.13.13